Acta Pharmaceutica Sinica B 2018;8(2):252–260

Chinese Pharmaceutical Association
Institute of Materia Medica, Chinese Academy of Medical Sciences

Acta Pharmaceutica Sinica B

www.elsevier.com/locate/apsb
www.sciencedirect.com

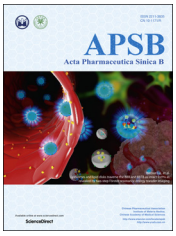

ORIGINAL ARTICLE

Comparative untargeted proteomic analysis of ADME proteins and tumor antigens for tumor cell lines

Xiaomei Gu[a], Qing Xiao[b], Qian Ruan[a], Yuezhong Shu[a], Ashok Dongre[b], Ramaswamy Iyer[a], W. Griffith Humphreys[a], Yurong Lai[a,*]

[a]*Pharmaceutical Candidate Optimization, Bristol-Myers Squibb Company, Princeton, NJ 08540, USA*
[b]*Genomics, Bristol-Myers Squibb Company, Princeton, NJ 08540, USA*

Received 17 July 2017; received in revised form 14 September 2017; accepted 16 September 2017

KEY WORDS

Cancer cell lines;
Untargeted quantitative proteomics;
Tumor-associated membrane proteins;
Cytochrome P450;
ABC transporters;
SLC transporters

Abstract In the present study, total membrane proteins from tumor cell lines including HepG2, Hep3B2, H226, Ovcar3 and N87 were extracted and digested with γLysC and trypsin. The resulting peptide lysate were pre-fractionated and subjected to untargeted quantitative proteomics analysis using a high resolution mass spectrometer. The mass spectra were processed by the MaxQuant and the protein abundances were estimated using total peak area (TPA) method. A total of 6037 proteins were identified, and the analysis resulted in the identification of 2647 membrane proteins. Of those, tumor antigens and absorption, metabolism, disposition and elimination (ADME) proteins including UDP-glucuronosyltransferase, cytochrome P450, solute carriers and ATP-binding cassette transporters were detected and disclosed significant variations among the cell lines. The principal component analysis was performed for the cluster of cell lines. The results demonstrated that H226 is closely related with N87, while Hep3B2 aligned with HepG2. The protein cluster of Ovcar3 was apart from that of other cell lines investigated. By providing for the first time quantitative untargeted proteomics analysis, the results delineated the expression profiles of membrane proteins. These findings provided a useful resource for selecting targets of choice for anticancer therapy through advancing data obtained from preclinical tumor cell line models to clinical outcomes.

*Corresponding author. Current address: Drug Metabolism, Gilead Sciences, 333 Lakeside Dr. Foster City, CA 94404, USA.
E-mail address: yurong.lai@gilead.com (Yurong Lai).

Peer review under responsibility of Institute of Materia Medica, Chinese Academy of Medical Sciences and Chinese Pharmaceutical Association.

http://dx.doi.org/10.1016/j.apsb.2017.10.002

1. Introduction

Cancer is the second most common deaths worldwide following heart disease and causes about 580,000 deaths per year in the United States[1]. Cancer therapy remains very challenging by struggling with the need to target and kill malignant cells while minimizing undesired collateral toxicity to normal tissue[2]. Over the last a few decades, human cancer cell lines become indispensable preclinical oncology models to study cancer cell functions and are frequently used to optimize therapeutic effects for new candidates of anticancer drugs. Cytotoxic reagents developed for chemotherapy have been introduced during past a few decades. However, they are mostly of limited clinical utility because the cytotoxicity toward both normal and malignant cells[3]. Multidrug resistance (MDR) has been a major issue in which malignant cells develop cross-resistance to chemotherapy cytotoxic drugs. Multidrug ATP-binding cassette (ABC) transporters that are overexpressed in many types of tumors are recognized to play key roles in their MDR by extruding cytotoxic reagents out of the tumor cells[4]. As a result, overexpressed membrane transporters, receptors and tumor antigens become targets to achieve a more specific treatment or discover precision medicine for cancer therapy[5]. Recently, utilizing overexpressed membrane receptors as cancer-targeting agents to deliver a chemically or genetically conjugated toxic molecule has gained increasing attentions for the therapeutic efficacy[6,7]. Such ligand–drug conjugates or antibody drug conjugates (ADCs) that consist of monoclonal antibodies attached to biologically active drugs through chemical linkers[7]. For example, ADCs allow the discrimination between normal and malignant cells through specific bindings of antibodies to tumor associated membrane antigens to deliver tumor-cell-killing cytotoxic drugs. The antibodies are designed to bind preferentially to membrane antigens of malignant cells at a relatively high density, and internalize in a manner that allows for release of the cytotoxic drug from the linker in the appropriate intracellular compartment, where the linker is cleaved and the cytotoxic drug is released. Unexpectedly, despite initially encouraging clinical results, ADCs encounter a number of challenges including inherent and acquired drug resistance[8]. For example, Mylotarg®, the first ADC drug approved, was withdrawn from the market because the post-marketing trials that are required for accelerated approval failed to verify the clinical efficacy[9]. In addition, cancer treated with ADCs can acquire drug resistance through the mechanisms either increased expression of efflux transporter proteins or reduced expression of the targeting antigens[8]. As most of the next-generation cytotoxic compounds including monomethyl auristatin E and maytansine, are substrates for multidrug resistance transporters such as P-glycoprotein[10], it is increasingly clear that resistance to ADCs likely overlaps the resistances to conventional mechanisms of small molecule anticancer agents[11]. Collectively, the sensitivity of cytotoxic agents to MDR mechanisms is now a factor that is included in consideration of an optimal payload for an ADC.

As aforementioned, membrane proteins expressed in cancer cells represent antigen targets of choice for antibodies of ADCs. Identifying membrane proteins in the tumor cell lines could improve our understanding of their biological function and increase our capability to translate *in vitro* and preclinical results to human. In addition, comprehensive profiling membrane proteins will facilitate our understanding of their critical roles in biological processes such as cell-to-cell adhesions, cell signaling, and solute transport across cellar membrane. Additionally, the analysis will increase our understanding of the biology for tumor cell lines in order to explain the difference in sensitivity to therapeutic reagents. Nevertheless, despite of their biological importance, the proteomic analysis of membrane proteins remains challenging. The ability to characterize membrane protein expression profiles has lagged behind that of soluble proteins both in terms of throughput and protein coverage. The low abundance and hydrophobic nature of membrane transporter proteins further complicate denaturing, digestion and identification by mass spectrometer[12].

Currently, numerous cancer cell lines representing the most cancer types found in human have been established. In the present investigation, five tumor cell lines were initially selected by considering our primary research efforts of ADC drug targets to elucidate drug resistance mechanisms observed in preclinical drug testing. An in-depth proteomic analysis of the membrane factions extracted from various tumor cell lines were carried out and our dataset encompass >6000 proteins with 2647 membrane bound proteins annotated from the total membrane preparations, which provide a comprehensive and quantitative repository for membrane proteomics data. While membrane proteome of the tumor cells tested is provided in the Supplementary material as a database for public access, the current analysis is focusing on the comparative analysis only for ADME and tumor antigen proteins. Comprehensive expression profiles of membrane proteins demonstrate quantitative differences in protein expression among tumor cell lines. The information could be used to bridge preclinical efficacy results obtained from the cell lines to *in vivo*, and therefore delineate targets of tumor associated proteins and potential pre-existing drug resistances to cytotoxic anticancer drugs.

2. Methods and materials

2.1. Chemicals and reagents

Cell culture reagents including Dulbecco's modified Eagle's medium, minimal essential medium, fetal calf serum, trypsin, Hank's balanced salt solution (HBSS), nonessential amino acids, and L-glutamine were purchased from Mediatech (Herndon, VA, USA). Biocoat poly-D-lysine–coated flask were purchased from BD Biosciences (Bedford, MA, USA). Formic Acid (FA), Dithiothreitol (DTT), Iodoacetamide (IAA), ammonium bicarbonate, ammonium acetate, urea, sodium bicarbonate and protease inhibitor were purchased from Sigma–Aldrich (St. Louis, MO, USA). Trypsin Gold (Mass Spectrometry Grade), and γLys/C (Mass Spec Grade) were from Promega Corporation (Madison, WI, USA). BCA protein assay kit was purchased from Pierce Chemical (Rockford, IL, USA). All other chemicals and reagents were purchased from Sigma–Aldrich (St. Louis, MO, USA). Human ovarian cancer cell lines OVCAR3, the human squamous cell carcinoma cell line H226, human hepatoma derived cell line HepG2, the human gastric cancer cell line N87 and the human hepatoma cell line Hep3B2 were obtained from American Type Culture Collection. The cells were maintained as recommended by vendor. Solvents and reagents were purchased from commercial manufacturers and were of analytical or HPLC grade.

2.2. Cell culture for tumor cells

The human Hep3B2 hepatoma cell lines were cultured in MEM supplemented with 10% fetal bovine serum (FBS) and penicillin–streptomycin (100 U/mL). OVCAR3, H226, N87 and HepG2 cells

were grown in RPMI 1640 medium with 10% FBS and 1% penicillin-streptomycin. Tissue culture plates or flasks were incubated at 37 °C with a humidified 5% CO_2 atmosphere. Cell growth and morphology was monitored for a period of 24 to 72 h post-seeding.

2.3. Extraction of membrane protein of tumor cells

The membrane protein fraction was extracted from minimum 20 million cells using the native membrane protein extraction kit (EMD Millipore (Calibiochem), Bellirica, MA, USA) as previously described[13]. The membrane extraction kit has been validated to demonstrate the high extraction efficiency and consistent yield[14–19]. Briefly, the cells were washed two times with washing buffer, and then lysed in the extraction buffer I in the kit containing the appropriate amount of protease inhibitor cocktail. After incubated at 4 °C for 30 min in a rotary shaker, the cell lysates were centrifuged at 16,000 × *g* (Eppendorf 5810r, Eppendorf North America, Hauppauge, USA) for 15 min at 4 °C. The supernatant containing cytosolic proteins was discarded and the pellets were re-suspended in extraction buffer II containing the proper amount of protease inhibitor cocktail. After a 30 min incubation at 4 °C, the suspension was centrifuged at 16,000 × *g* for 15 min at 4 °C. The supernatant that membrane fraction enriched integral membrane and membrane associated proteins was transferred into a new 2-mL Eppendorf centrifuge tube (Eppendorf of North American, Hauppauge, NY, USA). The protein concentration of the membrane fractions were determined by a BCA protein assay according to the manufacturer's instructions and the samples were stored at –80 °C for future analysis.

2.4. Purification of membrane proteins

Precipitation ProteoExtract Kit (EMD Millipore (Calibiochem), Bellirica, MA, USA) was used to purify the membrane fraction obtained above by removing the detergent contained in the membrane extraction buffer II of native membrane protein extraction kit, according to the vendor's protocol. In brief, membrane protein (200 μg) in the buffer II was mixed with four volume of cold precipitation agent (−20 °C) in a 2-mL Eppendorf LoBind centrifuge tube and vortexed briefly. The mixture was incubated for 20 to 60 min at −20 °C, and then centrifuged at 10,000 × *g* for 10 min at room temperature to precipitate the protein. The supernatant was carefully removed and the protein pellet was washed three times with 500 μL cold wash solution (−20 °C). The protein pellet was dried by leaving the open tube on the lab bench for up to 1 h at room temperature.

2.5. Denaturation and digestion of membrane protein samples

The air-dried protein pellet was re-dissolved in 50 μL of fresh prepared 8 mol/L urea/ 0.4 mol/L ammonium bicarbonate solution, vortexed and sonicated if necessary. The protein was reduced with 5 μL (or 1/10 *v*:*v*) of 45 mmol/L DTT at 50 °C for 15 min and then alkylated with 5 μL of 100 mmol/L iodoacetamide in dark at room temperature for 15 min. γLys/C enzyme was added to each sample at 1:100 enzyme to protein ratio (by weight) and incubated at 37 °C for 3 to 4 h. After diluted with about 138 μL H_2O (total volume of 200 μL), trypsin was then added to each sample at a 1:25 trypsin to protein ratio and incubated at 37 °C for 24 h. The digestion was stopped by adding 2 μL of formic acid. The sample was then centrifuged at 16,000 × *g* at room temperature for 10 min. To clean up the samples, 200 μL supernatant was transferred into a MacroSpin™ column (The Nest Group, Inc., MA, USA) that is preconditioned followed by vendor's instruction. The column was centrifuged at 110 × *g* for 1 min and washed twice with 100 μL H_2O. The digested peptides on the column were eluted with 50 μL of 80% acetonitrile containing 0.1% formic acid for two times and the eluent was combined for MS analysis.

2.6. Preparative HPLC for sample fractionation

Fractionation of the digested samples was achieved in an integrated Agilent 1100 HPLC series system with an Agilent ZORBAX 300 Extend-C18 column (150 mm × 2.1 mm, 3.5 μm). Mobile phase buffer A was 10 mmol/L ammonium formate (pH = 10), and buffer B contained 10% buffer A/90% ACN. Elution was achieved using multiple-step gradient with increasing proportions of buffer B: 0 min, 2% B; 4 min, 10% B; 44 min, 30% B; 54 min, 40% B; 56 min, 90% B; 58.1 min, 2% B; 70 min stop. The column mobile phase flow rate was 200 μL/mL. Total 60 factions were collected per run with one fraction isolated per 1 min collected from 4 to 64 min. After collection, a total of 12 fractions were generated by concatenating every 6th fractions in the collection plate and then dried in speed Vac overnight to dryness. The samples were reconstituted in 100 μL 10% ACN in water containing 0.1% formic acid.

2.7. LC/MS analysis for membrane protein

For the proteomic detection, the fractionated digested peptide mixtures were chromatographically separated on Shimadzu LC30 AD HPLC system. 100 μL sample was injected on an Acquity UPLC® BEH peptide C18 column (300 Å, 150 mm × 2.1 mm, 1.7 μm, Waters, MA, USA) with column temperature maintained at 60 °C, and elution of the digested peptides was achieved using a 120 min gradient (2% to 30% B from 5–100 min, then 30% to 95% ACN over 10 min, and equilibrating column back to original condition). The elution flow rate was 200 μL/min. Mobile phase buffer A was 0.1% formic acid in water and the buffer B was 0.1% formic acid in acetonitrile.

The Q-Exactive instrument (ThermoFisher Scientific, Waltham, MA, USA) was operated using full scan (survey scan) followed by a data dependent top-10 MS/MS scan. The full scan was achieved

Table 1 Instrument parameters.

Parameter	Setting
Full MS scan range	300–2000 Da
MS/MS fixed first mass	100 Da
AGC	$1e^6$, full scan $1e^5$, ms/ms
Max injection time	50 ms, full scan 100 ms, ms/ms
Isolation window	3.0 Da
NCE	28
Dynamic exclusion	30 s

AGC, Automatic gain control; NCE, Normalized collision engery.

at 70 K resolution at *m/z* 200, and the MS/MS scan was conducted at 17.5 K resolution for high energy collisional dissociation (HCD). Detailed instrument parameters are listed in Table 1. The Q-Exactive mass spectrometer was tuned and calibrated using a standard procedure and calibration solution recommended by the manufacture. The electrospray source was operated in the positive (+3.75 kV spray voltage) modes with heated-capillary temperature of 250 °C. High-purity nitrogen was used as the sheath and auxiliary gas and UHP helium was used as the dampening gas. The nitrogen gas flow rate, spray current, and voltages were adjusted to give maximum sensitivity.

2.8. *Data analysis*

From the resulting MS and MS/MS raw data, protein identification and quantification are achieved by database searching with MaxQuant software version 1.5.0.12 against a UniProt Knowledgebase Human Complete Proteome Sequence (http://www.uniprot.org/, March 2015). Peptides are identified from the acquired MS/MS spectra by peptide fragment-matching against spectra derived *in silico* from the protein sequence database. Carbamidomethylation of cysteines in digested peptides was set as fixed modification, while N-terminal acetylation and methionine oxidation were set as variable modifications. The maximum false discovery rate for peptides and protein were both specified as 0.01. Based on their cellular locations, identified proteins were annotated by gene ontology (GO) and assigned into four distinct categories including plasma, mitochondrial membrane, endoplasmic reticulum membrane and nuclear membrane. Peptide identities and relative intensities are then assigned to the corresponding protein properties. At the same time, precursor ion isotopic profiles are extracted around their chromatographic retention times, and their integrated peak areas are used for relative quantification of membrane proteins. In order to compare protein abundance across the five cell lines, missing protein intensities were imputed with a global minimum of all protein intensities divided by an arbitrary factor of 3. We then calculated intensity ratios of membrane proteins in each cell line using protein intensities in HepG2 as common denominators.

In order to further interrogate downstream statistical evaluation of the MaxQuant processing results obtained from 2–3 replicate injections, Perseus software (version 1.5.0.8) is then used to conduct sample-to-sample comparison, principal component analysis and hierarchical clustering. Protein intensities were log2-transformed, median-centered, and missing values were inputted from normal distribution with a width of 0.3 and down-shift of 1.8. A Benjamini–Hochberg false discovery ratio of 0.01 was used as a measure of statistical significance.

3. Results

3.1. *Experiment workflow and membrane protein proteomes of tumor cell lines*

As proteomics samples tend not to be analyzed as full length proteins in a LC/MS, protein mixtures are first subjected to enzymatic digestions. However, the challenges are often confounded by drastically increasing the number of enzymatically digested peptides in a mixture. With that in mind, based on the purpose to obtain a global picture of the membrane proteomes, the experimental procedure showed in Fig. 1 started to extract total membrane fractions from lysed tumor cells to maximally eliminate the interference of other components in the lysate. Followed by the sample cleaning, the protein mixtures were then performed enzymatic digestion with γLys/C and trypsin. In addition, salts and buffers in the resulting peptide mixtures were removed by a Macrospin™ column after enzymatic digestion and the resulting peptide mixtures were further pre-fractionated by an HPLC. Proteomics studies were accomplished using full scan in fractionated trypsin digest samples followed by data dependent top-10 MS/MS scan. The MS/MS scan was carried out at 17.5 K resolution for HCD and the resulting raw data were subjected to protein identification and quantification through database searching using MaxQuant software. As a result, a total of 6037 proteins along with 2647 membrane proteins were identified and quantified in the tumor cell line samples (Table 2), of which 96% (5799 proteins) were matched with at least two unique peptides.

Cell compartment annotations were further performed by GO, which is a useful tool to study protein composition of organelle membranes such as mitochondria. The isolation of the subcellular fractions of the tumor cell lines resulted in the identification of a total of 1640 plasma, 555 mitochondrial, 666 endoplasmic reticulum and 204 lysosomal membrane proteins in the tumor cell lines studied. Furthermore, intensity ratios of each protein in each of the cell line were calculated using the protein intensities in

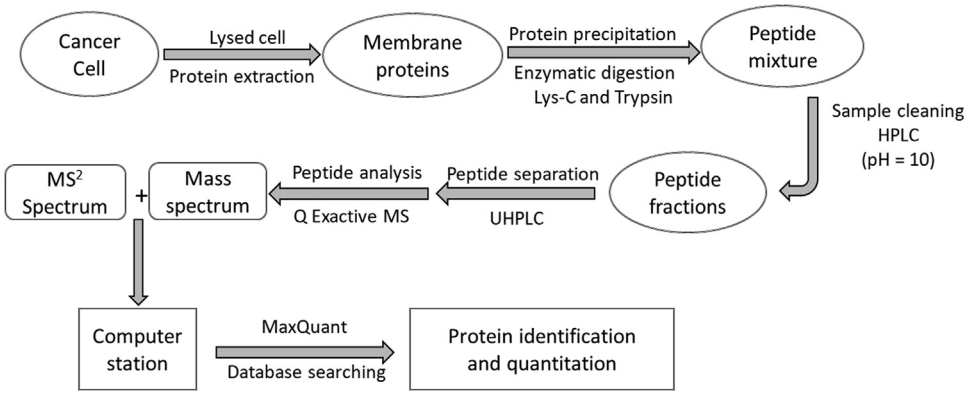

Figure 1 Experimental workflow. The main steps of membrane protein isolation, membrane protein purification, enzymatic digestion, mass-spectrometric data acquisition and protein identification and quantitation analysis are shown.

Table 2 Proteomics results of cancer cell membrane proteins.

Parameter	Cell Line					Total
	H226	Hep3B2	HepG2	N87	Ovcar3	
Number of proteins	5457	5149	5267	5554	5122	6037
ATP binding cassette transporters	31	34	34	32	29	36
Solute carriers	137	145	150	146	133	166
Cytochrome P450	9	11	15	14	13	18
UDP-glucuronosyl transferase	5	8	8	5	4	10

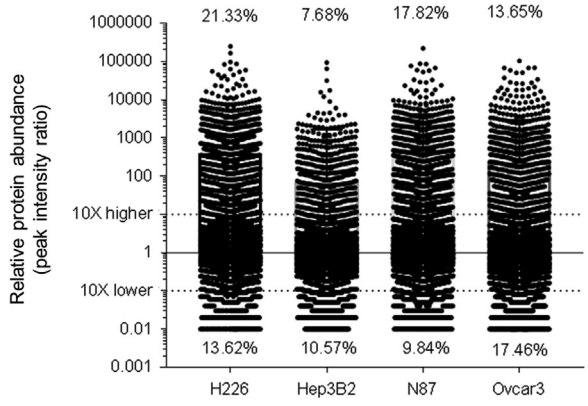

Figure 2 Expression of membrane proteins in each tumor cell line using HepG2 expression as Denominator. The membrane expression in HepG2 cells was set to 1 (the hard line) and the dot lines represent the cutoffs of protein expression at 10-fold lower or higher than HepG2 cells. The percentages in the figure represent the proteins of total protein numbers detected that are 10 fold lower or higher than that in HepG2 cells.

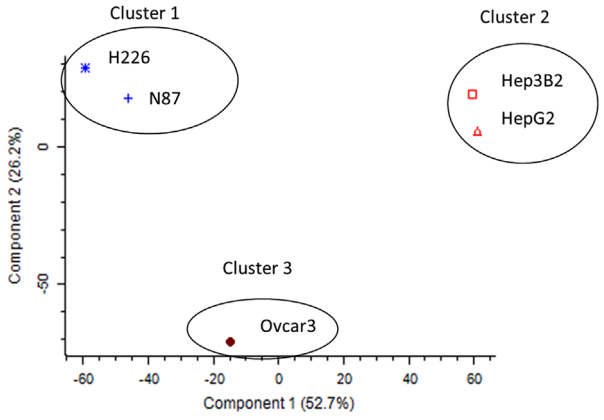

Figure 3 Principal component analysis (PCA) was performed on protein expression profiles of the 5 cell lines, and revealed 3 distinct clusters. H226 was closely clustered together with N87 (cluster 1), while Hep3B2 was clustered together with HepG2 (cluster 2). Ovcar3 was clustered separately (cluster 3).

HepG2 as common denominators. The analysis demonstrated significant variations in membrane protein expression among the tumor cell lines. As depicted in Fig. 2, approximately 21.33%, 7.68%, 17.82% and 13.65% of the total number proteins detected in H226, Hep3B2, N87 and Ovcar3 cells respectively were 10-fold greater, while about 13.62%, 10.57%, 9.84% and 17.46% of total number proteins appeared to be 10-fold lower than that in HepG2 cells. A table with full list of proteins annotated and their relative expressions to HepG2 cells is provided in the Supplementary Information table. Principal component analysis (PCA) was further performed on protein expression profiles of the 5 cell lines, and revealed 3 distinct clusters. H226 was closely clustered together with N87 (cluster 1 in Fig. 3), while Hep3B2 was clustered together with HepG2 (cluster 2 in Fig. 3). In contrast, Ovcar3 appeared to be clustered separately (cluster 3 in Fig. 3). Interestingly, HepG2 and Hep3B2 are both originated from human hepatocarcinoma cells and share the same cluster (Fig. 3).

3.2. Expression profiles of tumor-associated membrane proteins (TAMPs)

In order to examine the function of proteins detected, annotation according to GO was performed. As showed in Fig. 4, various tumor associated membrane proteins (TAMPs) have GO annotations and disclose significant variations in expression profiles among the cell lines tested. Of those, H226 cells were found to highly express tissue factor, mesothelin (MSLN), Zinc transporter (Zip6), trophoblast glycoprotein (TPBG), epidermal growth factor receptors (EGFR), fibronectin type III domain-containing protein B (FNDC3B), CD44 antigen (CD44), ephrin type-A receptor 2 (EpHA2), insulin-like growth factor 1 receptor (IGF1R), urokinase plasminogen activator surface receptor (PLAUR) and hepatocyte growth factor receptor (MET), while the expressions of poliovirus receptor-related protein 4 (PVRL4), arcinoembryonic antigen-related cell adhesion molecule (CEACAM), ectonucleotide pyrophosphatase/phosphodiesterase family member 3 (ENPP3), folate receptor 1 (FOLR1), neural cell adhesion molecule 1 (NCAM1), mucin-1 (MUC1) and tumor-associated calcium signal transducer 2 (TACSTD2) were minimal in the cells. In contrast, N87 highly expressed receptor tyrosine-protein kinase erbB-2 (ERBB2), CEACAM5 and cadherin (CDH3). Additionally, TACSTD2, tissue factor, MSLN, EGFR, glypican-3 (GPC3) and FNDC3B were also expressed in N87 cells at a lower level. HepG2 cells highly expressed GPC3, ENPP3 and CEACAM1, but not CEACAM5 and CEACAM6, while Hep3B2 cells were found to express GPC3, FNDC3B, epithelial cell adhesion molecule (EPCAM) and EGFR at a lower level than other cell lines (Fig. 4). Ovcar3 cells highly expressed neural cell adhesion molecule 1 (NCAM1), TACSTD2 and mucin1 (MUC1). Lower level expressions of EGFR, MSLN, ERBB2, EPCAM, EpHA2 and FNDC3B were also found in Ovcar 3 cells.

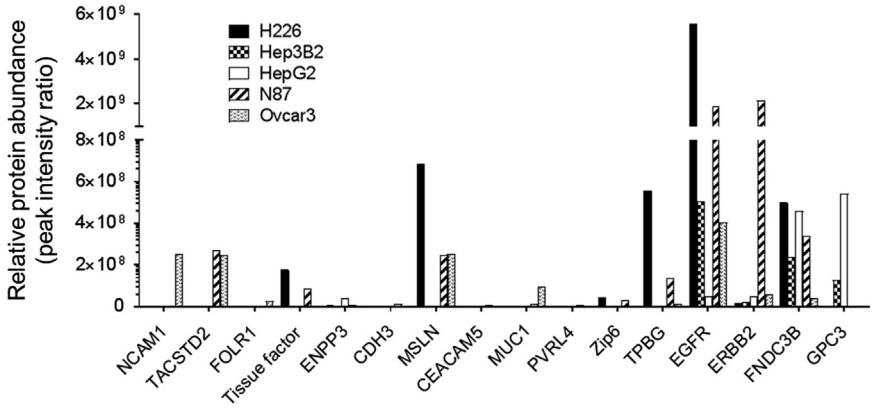

Figure 4 Expression of tumor-associated membrane proteins (TAMPs). Protein identification and quantification are achieved by database searching with MaxQuant software using MS and MS/MS raw data against a UniProt Knowledgebase Human Complete Proteome Sequence. Peptides are identified from the acquired MS/MS spectra by peptide fragment-matching against spectra derived *in silico* from the protein sequence database. The identified proteins were annotated by gene ontology (GO). TAMPs in the tumor cell lines tested were plotted by relative protein abundance. NCAM1: neural cell adhesion molecule 1; TACSTD2: tumor-associated calcium signal transducer 2; FOLR1: folate receptor 1; ENPP3: ectonucleotide pyrophosphatase/phosphodiesterase family member 3; CDH3: cadherin; MSLN: mesothelin; CEACAM5: carcinoembryonic antigen related cell adhesion molecule 5; MUC1: mucin 1; PVRL4: poliovirus receptor-related protein 4; Zip6: zinc transporter 6; TPBG: trophoblast glycoprotein; EGFR: epidermal growth factor receptors; ERBB2: receptor tyrosine-protein kinase erbB-2; FNC3B: fibronectin type III domain-containing protein B; GPC3: glypican-3.

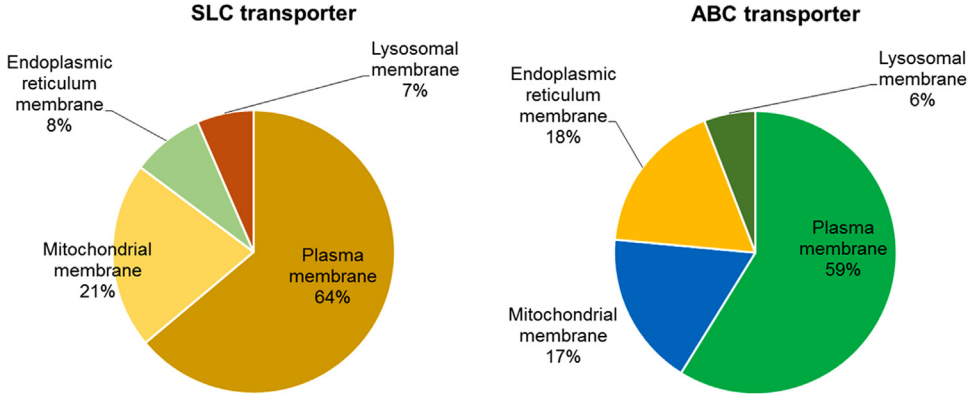

Figure 5 Subcellular localization of membrane transporter proteins in the tumor cells. The identified transporter proteins were annotated by gene ontology (GO). According to the GO annotation, the localization of membrane proteins detected by untargeted proteomics analysis was assigned into four distinct categories including plasma, mitochondrial membrane, endoplasmic reticulum membrane and nuclear membrane. The percentage in the chart represents the transporter proteins compared to the total membrane transporter numbers detected in the cell line.

Table 3 Intensity ratios of ABC transporter proteins in each cell lines using protein intensities in HepG2 as common denominators.

Symbol	Protein name	H226	Hep3B2	HepG2	N87	Ovcar3
ABCB1	Multidrug resistance protein 1 (MDR1-P-gp)	0.003	0.495	1.000	0.012	0.007
ABCB11	Bile salt export pump (BSEP)	LLQ	LLQ	1.000	LLQ	LLQ
ABCC1	Multidrug resistance-associated protein 1 (MRP1)	1.008	0.404	1.000	0.953	0.631
ABCC10	Multidrug resistance-associated protein 7 (MRP7)	0.200	0.204	1.000	0.231	0.168
ABCC2	Canalicular multispecific organic anion transporter 2 (MRP2)	0.010	0.548	1.000	0.042	0.013
ABCC3	Canalicular multispecific organic anion transporter 3 (MRP3)	0.028	0.334	1.000	0.431	0.039
ABCC4	Multidrug resistance-associated protein 4 (MRP4)	11.349	1.603	1.000	7.145	0.255
ABCC5	Multidrug resistance-associated protein 5 (MRP5)	6.069	1.051	1.000	2.736	0.233
ABCC6	Multidrug resistance-associated protein 6 (MRP6)	N/D	0.108	1.000	N/D	N/D
ABCG2	ATP-binding cassette sub-family G member 2 (BCRP)	28.502	2.963	1.000	0.376	0.024

Table 4 Intensity ratios of major SLC transporter proteins in each cell lines using protein intensities in HepG2 as common denominators.

Symbol	Protein name	Substrate	H226	Hep3B2	HepG2	N87	Ovcar3
SLC15A3	Solute carrier family 15 member 3	Di- and tripeptides	3058	1.85	1.00	5879	1204
SLC16A2	Monocarboxylate transporter 8	T2, rT3, T3, T4	1390	1.85	1.00	630	4.17
SLC16A7	Monocarboxylate transporter 2	Actate, pyruvate, ketone bodies	1582	1601	1.00	500	4.17
SLC19A2	Thiamine transporter 1	Thiamine	0.10	1.60	1.00	0.06	0.10
SLC22A18	Solute carrier family 22 member 18	Chloroquine, quinidine	3314	3195	1.00	4215	2259
SLC22A5	Solute carrier family 22 member 5	Organic cations, L-carnitine	46	0.02	1.00	20	0.04
SLC22A9	Solute carrier family 22 member 9	Estrone sulfate	0.01	184	1.00	0.01	0.03
SLC29A1	Equilibrative nucleoside transporter 1 (ENT1)	Purine and pyrimidine nucleosides	1.14	2.70	1.00	1.41	0.26
SLC29A2	Equilibrative nucleoside transporter 2 (ENT2)	Purine and pyrimidine nucleosides and some nucleobases	1.06	5914	1.00	1.09	331
SLC29A3	Equilibrative nucleoside transporter 3 (ENT3)	Purine and pyrimidine nucleosides and some nucleobases	0.00	0.16	1.00	0.07	0.00
SLC47A1	Multidrug and toxin extrusion protein 1	Organic cations	2.63	5.48	1.00	0.94	0.02
SLCO3A1	Solute carrier organic anion transporter family member 3A1	Estradiol-3-sulfate, prostaglandin	4740	1.85	1.00	2151	746

3.3. *Expression of membrane transporters*

The membrane proteomics analysis yielded a total of 166 solute carrier (SLC) proteins and 36 ABC transporter proteins (Table 2). Of those, a total of 108, 36, 14 and 11 SLC transporters and 20, 6, 6 and 2 ABC transporters were detected and annotated on plasma, mitochondria, endoplasmic, and lysosomal membrane, respectively (Fig. 5). ABC transporter expressions appeared to be significantly variable among the tumor cell lines. Table 3 summaries the major efflux transporters known to be associated to multidrug resistance. As showed in the Table 3, greater than 10-fold lower expression of MDR1-P-gp and multidrug resistance protein 2 (MRP2) were detected in H226, N87 and Ovcar3, as compared to HepG2 cells. MRP6 expression was found to be high in Hep3B2 and HepG2 cells. Interestingly, bile salt efflux pump (BSEP) was only found in HepG2 cells, but not in Hep3B2 cells, regardless of that Hep3B2 cells is similar to HepG2 cells, which both are originated from human hepatocellular carcinoma cells. The highest expression of BCRP was found in H226 cells, while BCRP in Ovcar3 cells was the lowest among the cell lines tested.

Table 4 summaries the major SLC transporters known to transport metabolites and therapeutic reagents. As shown in Table 4, the expression of SLC transporter proteins varied among the tumor cell lines. SLC15A3, a proton oligopeptide cotransporter was found to be highly expressed in H226, N87 and Ovcar3 cells, while the expressions in Hep3B2 and HepG2 were low. SLC16A2 and SLC16A7 that belong to the monocarboxylate transporter family and transport metabolites such as lactate, pyruvate and ketone bodies were highly expressed in H226, N87 and Hep3B2 (SLC16A7). On the other hand, thiamine transporter SLC19A2 was expressed at a low level in H226, N87 and Ovcar3 cells, as compared to that in HepG2 and Hep3B2 cells. The expression of SLC22A transporter family varied, as HepG2 cells were found to express the lowest level of SLC22A18 among the cell lines. SLC22A5 (organic cation/carnitine transporter 2, OCTN2) that transports many endogenous small organic cations as well as a wide array of drugs was highly expressed in human lung squamous H226 cells and human gastric carcinoma N87 cells. The high expression of SLC29A2 (equilibrative nucleoside transporter 2, ENT2) was found in human hepatocellular carcinoma Hep3B2 and human adenocarcinoma Ovcar3 cells, while SLC29A3 (ENT3) was found to be high in HepG2 cells. Interestingly, the expression of SLC29A1 (ENT1) was comparable among the cell lines tested. SLC47A1 that codes the multidrug and toxin extrusion protein 1 (MATE1) to excrete endogenous and exogenous electrolytes and drugs was found to be low in Ovcar3 cells. SLCO3A1 was the only gene detected in SLCO family. The expression of SLCO3A1 was high in H226 and N87 cells, as compared to other tumor cell lines.

4. Discussion

The ability to accurately and sensitively quantify membrane proteins that are expressed in tumor cell lines is a fundamental requirement to investigate the tumor specific markers for cancer-targeting therapy and drug resistance mechanisms to cancer killing reagents. Due to the vast array of unique proteins with extensive span of abundances range in a whole lysed biological sample, development of bioanalytical methods for mass spectrometric analysis remain challenging and require additional sample preparation steps to remove interferences such as buffers and salts. Peptides are identified from the acquired MS/MS spectra by peptide fragment-matching against spectra derived *in silico* from the protein sequence database in MaxQuant, which allows some flexibility of modification including maximum two missed cleavages, cysteine cabamidomethylation, methionine oxidation and N-terminal acetylation[20]. PCA uses feature abundance level across runs to transform and plot the abundance data in principal component spaces, which allows visualizing features that are "close together" appearing together on the PCA plot and *vice versa*. PCA analysis revealed 3 distinct clusters (Fig. 3). As such, protein expression features closed each other between H226 and N87, and Hep3B2 related to HepG2. In contrast, Ovcar3 had different profile features from other cell lines tested. In fact, while it is logical that HepG2 and Hep3B2 share the same cluster as both cell lines originated from human hepatocarcinoma cells, N87 gastric carcinoma cells and H226 non-small cell lung cancer cells were clustered together demonstrating that both response to the growth inhibition when exposed to Trastuzumad, suggesting the similarity of EGFR pathway in these cells[21].

The epidermal growth factor receptor family including the epidermal growth factor receptors (EGFR), receptor tyrosine-protein kinases (ErbBs), fibroblast growth factor (FGF) receptors, hepatocyte growth factor receptor (MET) and insulin-like growth factor (IGF) receptors are upregulated in neoplastic tissues. These receptors play a key role in cancer biology during tumor development and are considered as TAMPs. The proteins recently become very attractive tumor targets for therapeutic anticancer purposes[22]. According to the biological functions, TAMPs can be classified as receptors, cell adhesion or anchoring proteins, membrane associated enzymes, transporter proteins and glycosyl-phosphatidyl inositol anchors[22]. Generally, targeting anticancer therapy can be achieved through disrupting the processes of cancer development, or directing an attached cancer-killing drug to tumor cells through tumor specific antibodies, peptides or DNA/RNA aptamers that specifically bind to TAMPs[23,24]. For examples, EpHA2 is highly expressed in several cancer types and the expression is associated with worse patient survival[25,26]. Various therapeutic approaches that include monoclonal antibodies and RNA interferences are developed for targeting EpHA2 for cancer therapy. Nevertheless, although protein expression profiles of Hep3B2 and HepG2 cells were located in the same cluster, the TAMPs expressions in the cell lines varied, as HepG2 cells highly expressed CEACAM1, GPC3, IGF1R and ENPP3, while Hep3B2 highly expressed EPCAM (Fig. 4). On the other hand, MSLN was found in H226, N87 and Ovcar3 cells, of which the highest expression was detected in H226 cells. As a result, anetumab ravtansine, an ADC drug that consists of anti-mesothelin antibody and maytansionid tubulin inhibitor DM4 through a hindered disulfide linker demonstrates potent and selective cytotoxicity on Ovcar3 and H226 cells[27], which indicates that understanding the expressions of TAMPs in the tumor cells are essential for antibody-directed delivery of cytotoxic drug to cancer cells by ADCs. Collectively, the differential expression of TAMPs among the tumor cell lines could be used for selecting sensitive tumor cells as models to evaluate therapeutic candidates targeting tumors. Therefore, the comparative protein expression data should be included to interpret preclinical efficacy results and to apply for translating *in vitro* efficacy data obtained from the cell lines to *in vivo* tumor types.

Membrane-bound proteins including drug transporters and other ADME-related proteins such as cytochrome P450 and phase II enzymes play a key role in disposition of an anticancer drug. ABC transporter family such as the multidrug resistance 1 (MDR1-P-gp) and the breast cancer resistance protein (BCRP) are plasma membrane proteins, which are typical efflux transporters to extrude chemotherapeutic agents out of the cancer cells in a manner against concentration gradients using energy from the hydrolysis of ATP[28]. In the context, arguably ABC efflux transporter-related inherent or acquired drug resistances have been the mechanisms most studied. For example, BCRP is highly expressed in a number of human cancer cells including gastric carcinoma, hepatocellular carcinoma and colon cancer, and is considered the major causes of multidrug resistance[29]. A greater than 10-fold lower expression of MDR1-P-gp and multidrug resistance protein 2 (MRP2) were detected in H226, N87 and Ovcar3, as compared to that in HepG2 cells. Accordingly, the cell lines with lower MDR-P-gp and MRP2 are more sensitive to chemotherapy reagents that are substrates for the transporters. On the other hand, the SLC expressed in many tumor tissues are of particular importance for the accumulation of cytotoxic antitumor drugs, which could be a determinant factor for anticancer efficacy[30]. In general, cancer cells need more certain nutritional elements for an aggressive growth over normal cells, which often lead to the upregulation of carriers in cancer cells for their survival. Therefore, substantial differences of membrane transporter expressions likely exist between normal and tumor cells, as well as among different tumor types. For example, nucleoside transporters transport many anticancer nucleoside drugs and the clinical efficacy of the drugs relies on expression of the transporters mediating entry of the drugs[31]. The nucleoside analog gemcitabine is commonly used for pancreatic adenocarcinoma, and cellular uptakes of gemcitabine rely on the nucleoside transporter SLC28/29 family[32]. Accumulative evidences show that therapeutic effects of gemcitabine is strongly related to the expression of these nucleoside transporters[33,34]. SLC22A18 that is highly expressed all tumor cells except HepG2 acts as organic cation transporter to transport of chloroquine and quinidine-related compounds in kidney and has been identified as one of several tumor-suppressing sub-transferable fragments located in the imprinted gene domain of 11p15.5. As the region is an important tumor-suppressor gene region, alternation or mutation in the gene are associated with Beckwith–Wiedemann syndrome and many types of cancers[35]. In total, comparative membrane protein proteomics analysis in various tumor cells can be useful in understanding anticancer efficacy and drug resistances, targeting cancer therapy, as well as elucidating targets of choice as tumor marker proteins[36]. Subsequently, the expression profiles could be used for potential derived xenograft tissues to guide the selection of chemotherapy reagents for the best clinical outcomes.

In conclusion, quantitative proteomics analysis for tumor cell lines is useful for the discovery of new diagnostic/predictive biomarkers which might in turn lead to the identification of new potential drug targets. Furthermore, the results obtained could give a better understanding of drug resistance and be used for translation of the preclinical efficacy results to the clinic. Such mass spectrometric analyses are highly challenging, as pre-analytical preparation of samples is critical for robust and biologically relevant results. Here, we applied the comparative untargeted proteomics method to identify and quantify membrane proteins in cell lines. The proteomics analysis with the focusing on TAMPs demonstrated significant variations among the tumor cell lines. The observation will lead to a greater appreciation for the role of membrane proteins in tumor development and drug resistance, and present targets of choice as tumor marker proteins. The expression profiles will be useful for further elucidation of tumor-specific protein expression and molecular mechanisms of anticancer drug design. The membrane proteome for the tumor cell lines tested is now available in the Supplementary information for public access.

Acknowledgments

The authors wish to acknowledge Tongtong Liu, Yueping Zhang and Dr. Hong Shen for the help of cell culture and sample preparations.

Appendix A. Supporting information

Supplementary data associated with this article can be found in the online version at doi:10.1016/j.apsb.2017.10.002.

References

1. Heron M. Deaths: leading causes for 2010. *Natl Vital Stat Rep* 2013;**62**:1–96.
2. Guan XM. Cancer metastases: challenges and opportunities. *Acta Pharm Sin B* 2015;**5**:402–18.
3. Zhou Q, Chaerkady R, Shaw PG, Kensler TW, Pandey A, Davidson NE. Screening for therapeutic targets of vorinostat by SILAC-based proteomic analysis in human breast cancer cells. *Proteomics* 2010;**10**:1029–39.
4. Conseil G, Deeley RG, Cole SP. Polymorphisms of MRP1 (ABCC1) and related ATP-dependent drug transporters. *Pharmacogenet Genom* 2005;**15**:523–33.
5. Zhu FS, Chen XM, Huang ZG, Wang ZR, Zhang DW, Zhang X. Rofecoxib augments anticancer effects by reversing intrinsic multidrug resistance gene expression in BGC-823 gastric cancer cells. *J Dig Dis* 2010;**11**:34–42.
6. Cheong SJ, Lee CM, Kim EM, Uhm TB, Jeong HJ, Kim DW, et al. Evaluation of the therapeutic efficacy of a VEGFR2-blocking antibody using sodium-iodide symporter molecular imaging in a tumor xenograft model. *Nucl Med Biol* 2011;**38**:93–101.
7. Gibiansky L, Gibiansky E. Target-mediated drug disposition model and its approximations for antibody–drug conjugates. *J Pharmacokinet Pharmacodyn* 2014;**41**:35–47.
8. Loganzo F, Tan X, Sung M, Jin G, Myers JS, Melamud E, et al. Tumor cells chronically treated with a trastuzumab-maytansinoid antibody–drug conjugate develop varied resistance mechanisms but respond to alternate treatments. *Mol Cancer Ther* 2015;**14**:952–63.
9. Przepiorka D, Deisseroth A, Kane R, Kaminskas E, Farrell AT, Pazdur R. Gemtuzumab ozogamicin. *J Clin Oncol* 2013;**31**:1699–700.
10. Kovtun YV, Audette CA, Mayo MF, Jones GE, Doherty H, Maloney EK, et al. Antibody–maytansinoid conjugates designed to bypass multidrug resistance. *Cancer Res* 2010;**70**:2528–37.
11. Shefet-Carasso L, Benhar I. Antibody-targeted drugs and drug resistance—challenges and solutions. *Drug Resist Updat* 2015;**18**:36–46.
12. Schey KL, Grey AC, Nicklay JJ. Mass spectrometry of membrane proteins: a focus on aquaporins. *Biochemistry* 2013;**52**:3807–17.
13. Li N, Nemirovskiy OV, Zhang Y, Yuan H, Mo J, Ji C, et al. Absolute quantification of multidrug resistance-associated protein 2 (MRP2/ABCC2) using liquid chromatography tandem mass spectrometry. *Anal Biochem* 2008;**380**:211–22.
14. Li N, Zhang Y, Hua F, Lai Y. Absolute difference of hepatobiliary transporter multidrug resistance-associated protein (MRP2/Mrp2) in liver tissues and isolated hepatocytes from rat, dog, monkey, and human. *Drug Metab Dispos* 2009;**37**:66–73.
15. Kimoto E, Yoshida K, Balogh LM, Bi YA, Maeda K, El-Kattan A, et al. Characterization of organic anion transporting polypeptide (OATP) expression and its functional contribution to the uptake of substrates in human hepatocytes. *Mol Pharm* 2012;**9**:3535–42.
16. Qiu X, Bi YA, Balogh LM, Lai Y. Absolute measurement of species differences in sodium taurocholate cotransporting polypeptide (NTCP/Ntcp) and its modulation in cultured hepatocytes. *J Pharm Sci* 2013;**102**:3252–63.
17. Qiu X, Zhang H, Lai Y. Quantitative targeted proteomics for membrane transporter proteins: method and application. *AAPS J* 2014;**16**:714–26.
18. Wang L, Collins C, Kelly EJ, Chu X, Ray AS, Salphati L, et al. Transporter expression in liver tissue from subjects with alcoholic or hepatitis C cirrhosis quantified by targeted quantitative proteomics. *Drug Metab Dispos* 2016;**44**:1752–8.
19. Li N, Singh P, Mandrell KM, Lai Y. Improved extrapolation of hepatobiliary clearance from *in vitro* sandwich cultured rat hepatocytes through absolute quantification of hepatobiliary transporters. *Mol Pharm* 2010;**7**:630–41.
20. Cox J, Mann M. MaxQuant enables high peptide identification rates, individualized p.p.b.-range mass accuracies and proteome-wide protein quantification. *Nat Biotechnol* 2008;**26**:1367–72.
21. Patel DK. Clinical use of anti-epidermal growth factor receptor monoclonal antibodies in metastatic colorectal cancer. *Pharmacotherapy* 2008;**28**:31S–41S.
22. Boonstra MC, de Geus SW, Prevoo HA, Hawinkels LJ, van de Velde CJ, Kuppen PJ, et al. Selecting targets for tumor imaging: an overview of cancer-associated membrane proteins. *Biomark Cancer* 2016;**8**:119–33.
23. Gerber DE. Targeted therapies: a new generation of cancer treatments. *Am Fam Physician* 2008;**77**:311–9.
24. Ciavarella S, Milano A, Dammacco F, Silvestris F. Targeted therapies in cancer. *Biodrugs* 2010;**24**:77–88.
25. Pasquale EB. Eph receptors and ephrins in cancer: bidirectional signaling and beyond. *Nat Rev Cancer* 2010;**10**:165–80.
26. Tandon M, Vemula SV, Mittal SK. Emerging strategies for EphA2 receptor targeting for cancer therapeutics. *Exp Opin Ther Targets* 2011;**15**:31–51.
27. Golfier S, Kopitz C, Kahnert A, Heisler I, Schatz CA, Stelte-Ludwig B, et al. Anetumab ravtansine: a novel mesothelin-targeting antibody–drug conjugate cures tumors with heterogeneous target expression favored by bystander effect. *Mol Cancer Ther* 2014;**13**:1537–48.
28. Gillet JP, Gottesman MM. Mechanisms of multidrug resistance in cancer. *Methods Mol Biol* 2010;**596**:47–76.
29. Mao Q. Role of the breast cancer resistance protein (ABCG2) in drug transport. *AAPS J* 2005;**7**:E118–33.
30. Li Q, Shu Y. Role of solute carriers in response to anticancer drugs. *Mol Cell Ther* 2014;**2**:15.
31. Baldwin SA, Mackey JR, Cass CE, Young JD. Nucleoside transporters: molecular biology and implications for therapeutic development. *Mol Med Today* 1999;**5**:216–24.
32. Podgorska M, Kocbuch K, Pawelczyk T. Recent advances in studies on biochemical and structural properties of equilibrative and concentrative nucleoside transporters. *Acta Biochim Pol* 2005;**52**:749–58.
33. Nakahira S, Nakamori S, Tsujie M, Takeda S, Sugimoto K, Takahashi Y, et al. Pretreatment with S-1, an oral derivative of 5-fluorouracil, enhances gemcitabine effects in pancreatic cancer xenografts. *Anticancer Res* 2008;**28**:179–86.
34. Komori S, Osada S, Yoshida K. Novel strategy with gemcitabine for advanced pancreatic cancer. *ISRN Oncol* 2011;**2011**:936893.
35. Jung Y, Jun Y, Lee HY, Kim S, Jung Y, Keum J, et al. Characterization of SLC22A18 as a tumor suppressor and novel biomarker in colorectal cancer. *Oncotarget* 2015;**6**:25368–80.
36. Grixti JM, O'Hagan S, Day PJ, Kell DB. Enhancing drug efficacy and therapeutic index through cheminformatics-based selection of small molecule binary weapons that improve transporter-mediated targeting: a cytotoxicity system based on gemcitabine. *Front Pharmacol* 2017;**8**:155.